MICROMECHANICS OF RANDOMLY-GENERATED PARTICLE PACKS FOR DEM SIMULATIONS OF GRANULAR MATERIALS USING THE STRESS-FORCE-FABRIC RELATIONSHIP

Kamila Rodrigues Cassares Seko

Eduardo de Morais Barreto Campello

kamilacassares@usp.br

campello@usp.br

Department of Structural and Geotechnical Engineering, University of São Paulo

P.O. Box 61548, 05424-970, São Paulo, SP, Brazil

Abstract. *In this work we investigate the micromechanical properties of packs of particles using the stress-force-fabric (SFF) relationship. The packs are randomly generated using a particle-packing method recently proposed by the authors, and are at first characterized with respect to simple properties such as packing density, total number of contacts and coordination number. We then compute the packs´ fabric tensor, fabric anisotropy tensor, normal contact force tensor and tangential (friction) force tensor, such that their microstructure is further characterized w.r.t. granular fabric and principal contact directions. These features provide a good estimate to the degree of anisotropy of the packs and reveal their internal load-carrying structure, whereas at the same time also serve as indicators of "quality" of the adopted particle-packing method. The average stress tensor of each pack, relating inter-particle contact forces and directions to the bulk stress response of the pack (and thereby providing a direct relation between microscopic properties and macroscopic, continuum-like behavior), is also computed. This work presents partial results of a bigger research that is currently being conducted by the authors at Department of Structural and Geotechnical Engineering in University of São Paulo.*

Keywords: *Granular materials, Micromechanics, DEM, Stress-force-fabric relationship*

1 INTRODUCTION

The behavior of engineering materials is often described in terms of macroscopic characteristics. These are usually based on continuum quantities, such as stress and strain. Establishing stress-strain relationships in the form of constitutive equations to solve boundary value problems, with the aim to represent the mechanics of material behavior, is of great interest in engineering. In the particular case of granular materials (such as, but not limited to, soils), these techniques may be enhanced through the treatment of the material as an assembly of interacting particles, with contact forces, contact orientations and many other microscopic aspects.

Granular materials frequently exhibit a sophisticated collective behavior, though at the level of the individual grains they experience relatively simple inter-particle interactions. Knowledge on the micromechanics of these interactions may be used to establish a link between micro- and macro-level characteristics of such materials. In this sense, the mechanical behavior can be studied to a good extent by the fabric (microstructure) and spatial distribution of contact forces, this latter in both orientation and magnitude. Chang et al. in 1985, Darbre and Wolf in 1985, Rothenburg and Bathurst in 1989 and Emeriault and Cambou in 1996 are some examples of researchers that proposed analytical constitutive models for idealized granular assemblies (composed of spheres) with an assumed fabric structure (Ng, 1999).

Micromechanics of granular assemblies can be studied either by numerical and experimental techniques. These latter are usually time consuming when compared to the first, and sometimes subjective. They also have the drawback that it is hard to produce identical specimens with which statistical analysis of results can be satisfactorily performed. Thornton and Barnes in 1986 highlighted the possibility of visual analysis of the internal deformation processes throughout a computational simulation as a mean to gain insight into the physics of granular materials. In this work, we follow such an approach and adopt numerical techniques; specifically, we adopt the Discrete Element Method (DEM) to investigate the time evolution of granular particle systems.

Some works using DEM simulations of plane assemblies of discs are: Cundall and Strack (1979); Cundall et al. (1982); Thornton and Barnes (1986); Bathurst and Rothenburg (1989); Rothenburg and Kruyt (2004); Kruyt (2012). These are regarded as already classical works on the field. Ng (1999) studied the fabric of granular materials after compaction. For three-dimensional assemblies (spheres), important contributions are: Darbre and Wolf (1985); Emeriault & Cambou (1996); Thornton and Antony (1998); Ng (1999); Thornton (2000); Ng(2001); Ng(2004); Dorostkar & Mirghasemi(2015). The work of Emeriault and Cambou, in 1996, emphasized the importance of micromechanical approach in modelling anisotropic elastic behavior of granular materials and its applicability in soil analysis submitted to vibrations of very small amplitude cycles.

The DEM allows a computational model wherein the finite displacements and rotations of discrete interacting bodies (called discrete elements or particles) are tracked and computed in time. Throughout their motion, the particles come into contact with each other, and may lose contact too. These changes have to be identified and properly resolved. Specification of the initial conditions of the system (as well as occasional boundary conditions) is extremely important, as the response of a pack of particles (or granular assembly) is intrinsically dependent on this. Characteristics of the pack´s microstructure, like packing density, load level and fabric anisotropy, are extremely relevant to its collective mechanical behavior.

This paper uses the so-called stress-force-fabric (SFF) relationship proposed by Rothenburg and Bathurst (1989) to investigate the microstructure of randomly generated packs of particles. We employ concepts from statistical physics (like the theory of directional statistics) to study the macro stress state of granular materials starting from the level of the particle scale. Specifically, we use special microstructural parameters to measure the anisotropy of such packs. We believe that by having a thorough characterization of the packs´ microstructure we may identify initial trends to their macroscopic behavior (from a mechanistic point of view), and at the same time identify whereas the particle packing technique is biased towards any such microstructural aspect.

2 MICROMECHANICAL PROPERTIES OF GRANULAR MATERIALS

The coordination number, Z, is a scalar quantity that furnishes the average number of contacts per particle in a particle assembly. It is a measure of the contact density of the assembly, defined as

$$Z = 2\frac{N_c}{N_p}, \tag{1}$$

where N_c is the total number of physical contacts and N_p is the number of particles in the arrangement. It is necessary to highlight that Z does not give any information about orientations of interparticle contacts, contact forces magnitudes, particles´ shape and particle size. However, it is possible to show that the coordination number is related to the pack density (or, equivalently, to the void ratio).

The fabric tensor, in turn, is a measure of changes in the fabric of granular materials. This tensor is sometimes considered a measure of stress in a sample characterized by an induced anisotropy in contact normal orientations. In component form, the fabric tensor $\boldsymbol{R}$ is defined as

$$R_{ij} = \frac{1}{2N_c}\sum_{c=1}^{N_c} n_i^c n_j^c, \quad i, j = 1, 2, 3, \tag{2}$$

where n_i^c is the "i" component of the unit vector that describes the contact normal orientation of contact point c. As shown in Fig. 1, components of this vector in a spherical coordinate system may be written as:

$$n_1^c = \cos\beta \sin\gamma, \; n_2^c = \sin\beta\sin\gamma, \; n_3^c = \cos\gamma. \tag{3}$$

The deviatoric part of the fabric tensor, $\boldsymbol{R}'$, is

$$R'_{ij} = R_{ij} - \frac{\delta_{ij}}{3}, \tag{4}$$

where δ_{ij} is the Kronecker-delta.

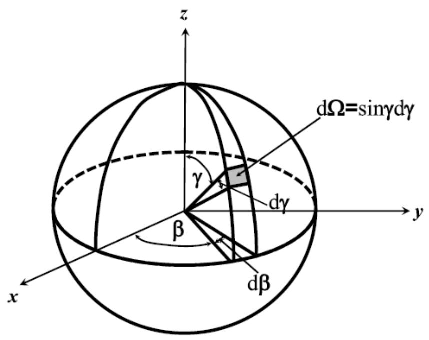

Figure 1. Spherical coordinates for unit contact normal definition

A particle pack usually shows anisotropy. This anisotropy may be classified into inherent, induced and initial. The inherent anisotropy is a consequence of the depositional process to form the pack. The geometry of particles strongly influences this kind of anisotropy. As discussed by Oda (1972), it happens even when spherical particles are used. We consider that this sort of anisotropy needs to be determined (or at least estimated) prior to performing any simulation with the pack – otherwise unrevealed microstructural characteristics may induce wrong conclusions on the macroscopic behavior of the pack.

It is possible to relate the anisotropy to preferential orientations of the particles in the assembly. These orientations can be depicted by means of a probability density function $E\left(\boldsymbol{n}\right)$, where $\boldsymbol{n}$ is the unit vector that describes an orientation. A good approximation of the contact orientation distribution is:

$$E(\boldsymbol{n}) = E_0\left(1 + a_{ij}^r n_i^c n_j^c\right), \tag{5}$$

where E_0 is defined as $\oint_{\Omega} d\Omega$, wherein Ω is the domain in which the distribution is defined.

For two-dimensional assemblies, Ω is a unit circle and thereby $E_0 = 2\pi$; for three-dimensional ones, Ω is the unit sphere such that $E_0 = 4\pi$.

Following a Fourier expansion, Rothenburg and Bathurst (1989) proposed the following approximation to the contact orientation distribution:

$$E(\boldsymbol{n}) = E_0\left(1 + a\cos\left(\theta - \theta_a\right)\right), \tag{6}$$

where a is a parameter defining the magnitude of the fabric anisotropy and θ_a defines the direction of the fabric anisotropy, or principal fabric direction.

Dorostkar and Mirghasemi (2015) presented the following approximation for 2D assemblies:

$$\begin{cases} E(\boldsymbol{n}) = \dfrac{1}{2\pi}\left(1 + a_{ij}^r n_i^c n_j^c\right) \\ a_{ij}^r = a_{ji}^r, \quad a_{ii}^r = 0 \end{cases}, \tag{7}$$

where a_{ij}^r are the components of the so-called tensor of anisotropy, given by

$$a_{ij}^{r} = \frac{15}{2} R'_{ij} \ . \tag{8}$$

If the distribution is uniform and isotropic, $E\left(\boldsymbol{n}\right) = 1/2\pi$ and $a_{ij}^{r} = 0$.

2.1 Contact Forces

The contact force magnitude in an assembly of particles varies from contact to contact. However, some regular trends are found when normal and tangential components of inter-particle forces are averaged over groups of contacts with similar orientations. Normally, maximum forces are associated with contact orientations close to the direction of maximum principal stress (here, we mean "stress" from a macroscopic perspective on the assembly). In the same way, minimum normal forces are related with contacts oriented along the minimum principal stress direction.

Similarly to previous section, the distribution of average normal contact force $\overline{f}^{n}\left(\Omega\right)$ is given by:

$$\begin{cases} \overline{f}^{n}\left(\Omega\right) = \overline{f}^{0}\left(1 + a_{ij}^{n} n_i n_j\right) \\ \quad a_{ij}^{n} = a_{ji}^{n}, \quad a_{ii}^{n} = 0 \end{cases}, \tag{9}$$

where $\overline{f}^{0}$ symbolizes the normal contact force averaged over groups of similar orientations for isotropic assemblies. In case of anisotropic arrangements, $\overline{f}^{0}$ is the average normal contact force when all groups are given equal weight and it is defined as:

$$\overline{f}^{0} = \frac{1}{4\pi} \int_{\Omega} \overline{f}^{n}\left(\Omega\right) d\Omega \, . \tag{10}$$

By analogy to the fabric tensor, the normal contact force tensor is given by:

$$F_{ij}^{n} = \frac{1}{4\pi} \sum \overline{f}^{n}\left(\Omega^{g}\right) n_i n_j \Delta\Omega^{g} \ , \tag{11}$$

where Ω^{g} is a partitioned group of the unit sphere (see Fig. 1).

In component form, the normal force anisotropy tensor is expressed as:

$$a_{ij}^{n} = \frac{15}{2} F'^{n}_{ij} , \tag{12}$$

where

$$F'^{n}_{ij} = F_{ij}^{n} - \frac{\overline{f}^{0}}{3} \, . \tag{13}$$

It is important to emphasize that average tangential forces for contacts oriented along principal stress directions is equal to zero. Additionally, forces on contacts of these orientations are normal to plane of contact.

Distribution of average tangential contact force $\overline{f}^t\left(\Omega\right)$ is given by:

$$\begin{cases} \overline{f}^t\left(\Omega\right) = \overline{f}^0\left[a_{ij}^t n_j - \left(a_{kl}^t n_k n_l\right) n_i\right] \\ \quad a_{ij}^t = a_{ji}^t, \quad a_{ii}^t = 0 \end{cases}. \tag{14}$$

We want to highlight that the contact force vector is the decomposed as the sum of a normal and tangential components. So, tangential contact force contribution could be calculated.

Tangential contact force tensor, in component form, is given by:

$$F_{ij}^t = \frac{1}{4\pi}\sum_{N^g} \overline{f}_i^t\left(\Omega^g\right) n_j \Delta\Omega^g . \tag{15}$$

In component form, tangential contact force anisotropy tensor is:

$$a_{ij}^t = 5\frac{F_{ij}^t}{\overline{f}^0} . \tag{16}$$

2.2 Stress tensor: calculation from contact forces

The calculation of stress tensor $\boldsymbol{\sigma}$ for a pack is possible from static equilibrium. The relationship between stress tensor and forces and vectors at contact points can be written as:

$$\sigma_{ij} = \frac{1}{V}\sum_{i,j=1}^{3} f_i^c l_j^c . \tag{17}$$

where V is the volume of sample, f_i^c are components of contact force vector (including normal and tangential forces), and l_j^c are components of branch vector. The branch vector is defined as a vector extending from the centroid of particle i to the centroid of particle j.

It is possible to expand the tensorial expression for 3D, stress tensor gives:

$$\boldsymbol{\sigma} = \frac{1}{V}\begin{pmatrix} \sum_{c=1}^{N_c,V} f_1^c l_1^c & \sum_{c=1}^{N_c,V} f_1^c l_2^c & \sum_{c=1}^{N_c,V} f_1^c l_3^c \\ \sum_{c=1}^{N_c,V} f_2^c l_1^c & \sum_{c=1}^{N_c,V} f_2^c l_2^c & \sum_{c=1}^{N_c,V} f_2^c l_3^c \\ \sum_{c=1}^{N_c,V} f_3^c l_1^c & \sum_{c=1}^{N_c,V} f_3^c l_2^c & \sum_{c=1}^{N_c,V} f_3^c l_3^c \end{pmatrix}. \tag{18}$$

2.3 Coefficients of Contact Normal Anisotropy from Fabric Tensor for two-dimensional idealizes granular system

According to Bathrust (1995), a contact distribution function can be written using no more than second-order term, so:

$$E\left(\theta\right) = \frac{1}{2\pi}\left[1 + a\cos 2\left(\theta - \theta_a\right)\right], \tag{19}$$

Proceedings of the XXXVIII Iberian Latin-American Congress on Computational Methods in Engineering
P.O. Faria, R.H. Lopez, L.F.F. Miguel, W.J.S. Gomes, M. Noronha (Editores), ABMEC, Florianópolis, SC, Brazil, November 5-8, 2017.

where a is the coefficient of anisotropy and θ_a is the direction of anisotropy. The coefficient of anisotropy a is given by:

$$a = \frac{4R_{12}}{R_{11} + R_{22}}. \tag{20}$$

The direction of anisotropy θ_a is defined as:

$$\theta_a = \frac{1}{2}\arctan\left(\frac{2R_{12}}{R_{11} - R_{22}}\right). \tag{21}$$

These equations are used to calculate the anisotropy of two-dimensional packs.

2.4 Analysis of Fabric Eigenvalues

The fabric tensor is difficult to interpret or "visualize" and recognizing the similarity with stress tensor may be the best place to start an analysis with (O'Sullivan, 2011). The principal stresses and their orientation can be determined from the stress tensor. Similarly, the preferred orientations and the magnitude of the anisotropy can be determined from known fabric tensor. The method to measure the magnitude of anisotropy is not yet completely developed. However, researches tend to use the eigenvalues of this tensor. In this work, we define that Φ_1 is the major fabric, Φ_2 is the intermediate fabric and Φ_3 is the minor fabric eigenvalues.

In three dimensions, a fully anisotropic fabric will be characterized by three distinct eigenvalues. A transversely anisotropic one will be described by two distinct eigenvalues.

For two-dimensional systems, Table 1 shows different equations to quantify the anisotropy.

Table 1. Two-dimensional systems: equations to quantify the anisotropy

Researchers	Anisotropy
Curray (1956)	$\frac{\Phi_1 - \Phi_3}{2}$
Thornton (2000)	$\Phi_1 - \Phi_3$
Ibraim et al. (2006)	$\frac{\Phi_1}{\Phi_2}$
Maeda (2009)	$Z\left(\Phi_1 - \Phi_3\right)$

Interpretation of anisotropy in three-dimensional assemblies becomes more elaborated. The quantification of anisotropy proposed by Barreto (2009) is

$$\Phi_d = \frac{1}{\sqrt{2}}\sqrt{\left(\Phi_1 - \Phi_2\right)^2 + \left(\Phi_2 - \Phi_3\right)^2 + \left(\Phi_3 - \Phi_1\right)^2}. \tag{22}$$

O'Sullivan (2011) highlighted that Kuo et al. used a similar expression in 1998.

3 NUMERICAL EXAMPLES

In the following, first we describe briefly the particle-packing technique that we used to generate particle packs (Campello; Cassares, 2015). We consider this procedure as simple and fast for generating particle packs at high packing ratios. Our technique consists in a generation of packs in a layer-by-layer fashion beginning from the bottom of a bulk domain until a desired total height is achieved. The bulk domain is defined a priori. We choose a rectangle for 2D packs and a prism for 3D packs. The positions of the particles in each new layer are treated as random variables whose values are sampled from underlying probability distribution functions (pdfs), following a random sequence addition (RSA) approach. After that a jamming force is activated and the motion reached by the particles is resolved through a DEM simulation. As consequence, the new layer settles down and interacts with the previous layer by mechanical contact. This procedure is repeated for new layers until the desired total height for the jammed pack is achieved.

The radii of the generated particles can either be the same for all particles or be sampled from ad-hoc pdfs. In this study, we choose a Gaussian distribution (mean value and standard deviation must be provided). It is necessary to highlight that we do not adopt a particle growth scheme in the jamming stage of our technique.

It is essential to control four aspects for the technique to attain density effectiveness and computational efficiency. They are: (1) the use of appropriate material parameters for the particles within the DEM simulations, so that the contacts and collisions due to the jamming forces result inelastic enough (it enforces the system to settle down very rapidly for each new layer and avoiding undesired bouncing of particles as well as high frequency motions, which would require small time steps to be resolved adequately); (2) the use of explicit time integration scheme to perform the DEM simulations (this improves computational efficiency); (3) the start of each new layer at moderate initial densities like $\overline{\phi} = 0.4$ in 2D pack and $\overline{\phi} = 0.25$ in 3D pack (this feature is inherited from the RSA algorithm); and (4) consideration of rotational motion with particle spin and inter-particle friction in the DEM simulations.

The technique can be implemented into a script code. It is summarized in the Algorithm 1 below.

Algorithm 1. Generation of particle packs

```
1.  Get bulk boundaries and domain data (shape and sizes)
2.  Get layers' properties (initial shape and sizes, initial density φ̄, particle size
    or particle size distribution, particles' material properties)
3.  Get desired height for the jammed pack
4.  Get jamming force data
5.  Get time integration data (time step size, simulation times)
6.  FOR i = 1,...,n_S (n_S = number of sets be generated) DO:
       FOR j = 1,...,n_P (n_P = number of packs in each set) DO:
          current height = 0
          WHILE (current height < desired height) DO
             Generate new layer on top of previous layer(s) via RSA
             Apply jamming force and run DEM simulation
             Compute current height
          END DO
       END DO
    END DO
```

We adopted a gravity force of magnitude g as the jamming pseudo force and considered some energy dissipation. This jamming pseudo force acts in the direction from top to bottom of the bulk domain. The following data are common for all examples: Mass density of the particles = 1000 kg/m3; Elasticity modulus and Poisson coefficient of the particles (needed to resolve contacts/collisions with our DEM solver): $E = 10^8$ N/m² and $\nu = 0.25$; Damping rate for contacts/collisions: $\xi = 0.1$; Coefficient of dynamic friction for contacts/collisions: $\mu_d = 0.2$; Magnitude of gravity force (jamming pseudo-force): $g = 2$ m/s²; Drag force constant: $c_D = 0.005$ N·s/m; Initial velocity and spin of each newly generated particle: $\boldsymbol{v}(0) = \boldsymbol{w}_i(0) = \boldsymbol{o}$; Time step size for the DEM simulations: $\Delta t = 0.0001$ s; Duration of the jamming stage for each newly generated layer (i.e., DEM simulation time): $t = 1.0$ s; Typical number of particles in a pack: $N_p = 1300$ (2D packs). More detailed information about the particle generation process can be found in Campello and Cassares (2015).

3.1 2D rectangular packs of congruent particles

In this example, rectangular packs are considered and these have base length $L = 1.0$ m and desired height $H_d = 0.5$ m. We adopted $r_i = 0.01$ m ($i = 1,...,N_p$) for all particles. The initial thickness of each layer is set to $h_{layer} = 0.2H_d$ and the initial packing ratio is $\bar{\phi} = 0.4$. Using these data, ten packs are generated by means of Algorithm 1. We show the results in Fig. 2; the corresponding final densities are depicted in Table 2; the coordination number, components of fabric tensor and eigenvalues of this tensor, and anisotropy parameters in Table 3; estimation of the anisotropy value using eigenvalues of fabric tensor in Table 5. We repeat the procedure and generate another ten packs but now not considering rotational motion during the simulations of compaction stages. The results are shown in Fig. 3, the final densities are depicted in Table 2; the coordination number, components of fabric tensor and eigenvalues of this tensor, and anisotropy parameters in Table 4; estimation of the anisotropy value using eigenvalues of fabric tensor in Table 6.

Table 2. Packing densities (ϕ) obtained for example 3.1

Pack	rotations ON	rotations OFF
1	0.854	0.813
2	0.854	0.838
3	0.854	0.841
4	0.863	0.830
5	0.854	0.838
6	0.864	0.837
7	0.853	0.840
8	0.863	0.839
9	0.892	0.846
10	0.862	0.846
mean	0.861	0.837
st. deviation	0.012	0.010
coef. variation	0.014	0.012

Table 3. Packing coordination number (Z), Fabric Tensor and Anisotropy obtained for example 3.1 (rotations ON)

Pack	N_c	Z	Φ_1	Φ_3	R_{11}	R_{22}	R_{12}	a	θ_a
1	2436	3.791	0.560	0.440	0.440	0.560	$2.740\text{x}10^{-4}$	0.241	-0.13°
2	2432	3.800	0.550	0.450	0.450	0.550	$-1.606\text{x}10^{-3}$	0.202	0.91°
3	2450	3.831	0.547	0.454	0.454	0.547	$-2.640\text{x}10^{-4}$	0.186	0.16°
4	2354	3.681	0.541	0.460	0.460	0.540	$-8.675\text{x}10^{-3}$	0.162	6.18°
5	2411	3.758	0.533	0.467	0.469	0.531	$-1.185\text{x}10^{-2}$	0.134	10.38°
6	2455	3.830	0.536	0.464	0.466	0.534	$-9.781\text{x}10^{-3}$	0.142	7.98°
7	2425	3.804	0.518	0.482	0.482	0.518	$2.247\text{x}10^{-4}$	0.073	-0.35°
8	2400	3.750	0.531	0.469	0.470	0.530	$7.601\text{x}10^{-3}$	0.122	-7.20°
9	2432	3.803	0.520	0.481	0.481	0.519	$-3.912\text{x}10^{-3}$	0.078	5.82°
10	2417	3.791	0.532	0.468	0.468	0.532	$-1.181\text{x}10^{-4}$	0.129	0.11°

Table 4. Packing coordination number (Z), Fabric Tensor and Anisotropy obtained for example 3.1 (rotations OFF)

Pack	N_c	Z	Φ_1	Φ_3	R_{11}	R_{22}	R_{12}	a	θ_a
1	2267	3.576	0.529	0.471	0.472	0.528	$7.793\text{x}10^{-3}$	0.117	-7.73°
2	2225	3.512	0.537	0.463	0.463	0.537	$2.990\text{x}10^{-3}$	0.148	-2.31°
3	2269	3.585	0.528	0.472	0.472	0.528	$-2.726\text{x}10^{-3}$	0.112	2.79°
4	2259	3.574	0.530	0.470	0.470	0.530	$4.576\text{x}10^{-4}$	0.120	-0.44°
5	2250	3.538	0.538	0.463	0.463	0.538	$-6.875\text{x}10^{-4}$	0.150	0.53°
6	2280	3.585	0.542	0.458	0.458	0.542	$-1.764\text{x}10^{-3}$	0.169	1.19°
7	2265	3.575	0.529	0.471	0.471	0.529	$1.623\text{x}10^{-3}$	0.116	-1.61°
8	2253	3.565	0.539	0.461	0.461	0538	$3.732\text{x}10^{-3}$	0.155	-2.77°
9	2280	3.593	0.545	0.455	0.455	0.545	$-7.316\text{x}10^{-3}$	0.182	4.64°
10	2263	3.572	0.536	0.464	0.464	0.536	$4.705\text{x}10^{-3}$	0.145	-3.72°

Table 5. Estimation of the anisotropy value using eigenvalues of fabric tensor for example 3.1 (rotations ON)

Pack	a	CURRAY(1956)	THORNTON(2000)	IBRAIM et al. (2006)	MAEDA (2009)
1	0.241	0.060	0.120	1.273	0.456
2	0.202	0.051	0.101	1.225	0.384
3	0.186	0.047	0.093	1.205	0.356
4	0.162	0.041	0.081	1.176	0.298
5	0.134	0.034	0.067	1.143	0.252
6	0.142	0.036	0.071	1.153	0.272
7	0.073	0.018	0.036	1.076	0.139
8	0.122	0.031	0.061	1.130	0.229
9	0.078	0.019	0.039	1.081	0.148
10	0.129	0.032	0.065	1.138	0.245

Table 6. Estimation of the anisotropy value using eigenvalues of fabric tensor for example 3.1 (rotations OFF)

Pack	a	CURRAY(1956)	THORNTON(2000)	IBRAIM et al. (2006)	MAEDA (2009)
1	0.117	0.029	0.059	1.124	0.209
2	0.148	0.037	0.074	1.160	0.261
3	0.112	0.028	0.056	1.119	0.201
4	0.120	0.030	0.060	1.128	0.214
5	0.150	0.038	0.075	1.162	0.266
6	0.169	0.042	0.085	1.185	0.304
7	0.116	0.029	0.058	1.123	0.207
8	0.155	0.039	0.077	1.168	0.276
9	0.182	0.045	0.091	1.200	0.326
10	0.145	0.036	0.073	1.157	0.259

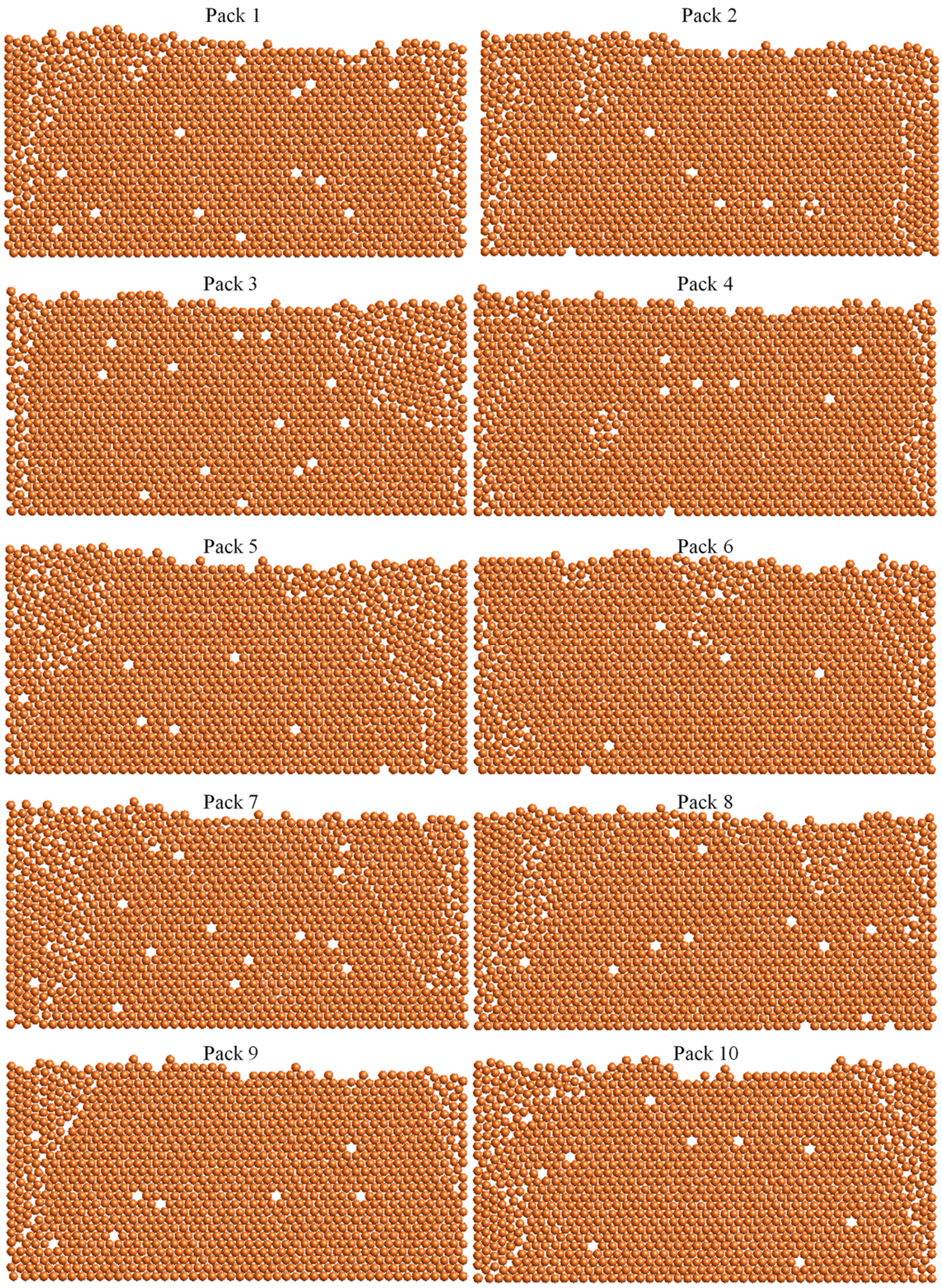

Figure 2. 2D packs of congruent particles (rotational motion is ON)

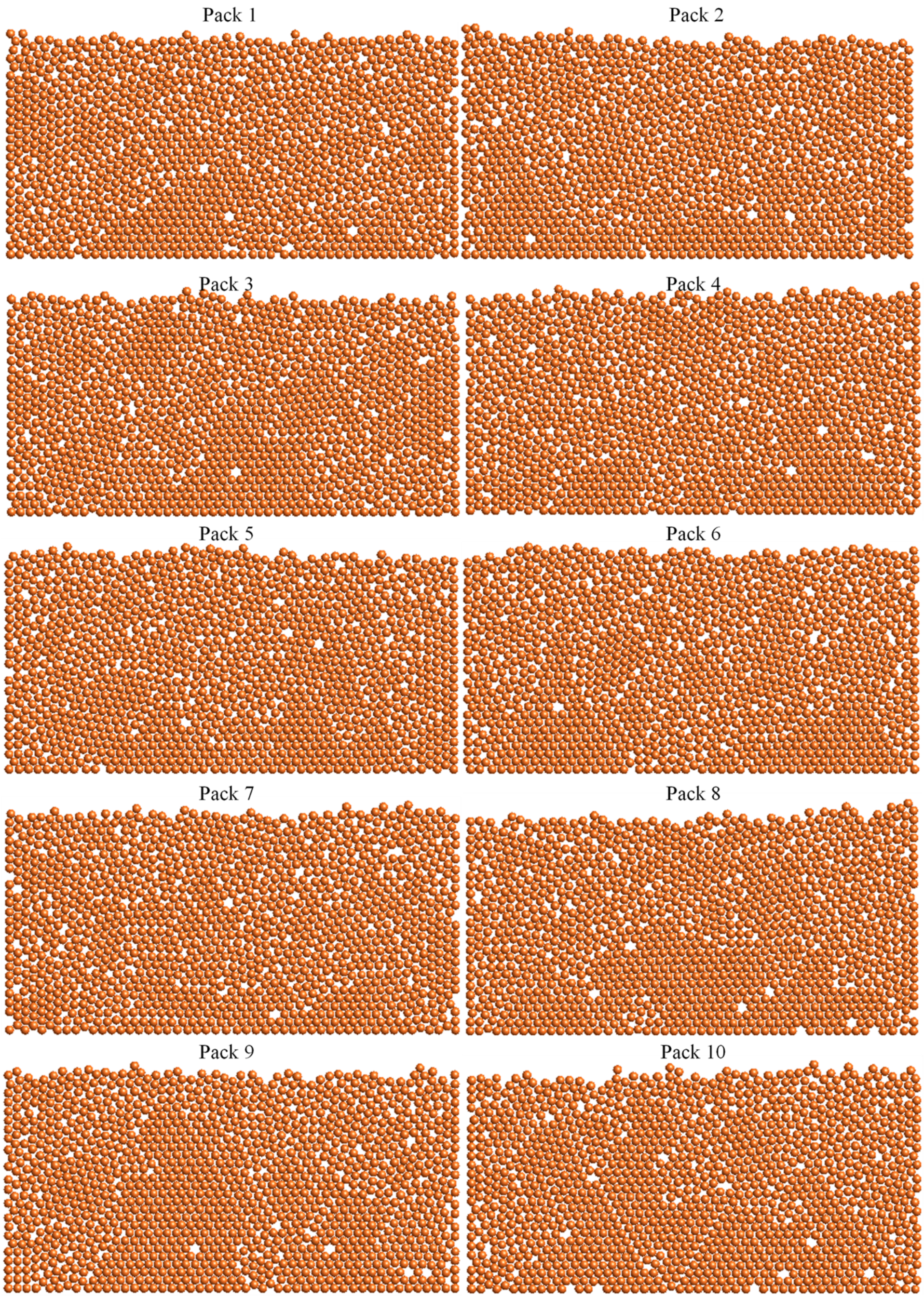

Figure 3. 2D packs of congruent particles (rotational motion is OFF)

We want to draw the attention to the results presented in Tables 3 and 4. It is possible to see that found values are similar. Therefore, the particles packs show more or less repeatable fabrics or microstructures.

It can be observed that the equation proposed by Thornton (2000) to quantify the anisotropy results is the half value of $|a|$ (Table 5 and Table 6). This approach was also adopted by Cui and O'Sullivan (2006) and the same consideration was made.

CONCLUSIONS

This work presents partial results of a bigger research about the fabric of 2D generated with our recently proposed packing generation algorithm. This research is currently being conducted by the authors at Department of Structural and Geotechnical Engineering in University of São Paulo. We want to emphasize that these packs of spherical particles were generated using a technique that, though very simple and fast, allows adequately high packing densities and more or less repeatable (yet randomly generated) fabrics or microstructures. This feature is extremely desirable if the packs are intended to serve as samples of granular materials on which DEM simulations are to be conducted, e.g. for material characterization purposes and/or determination of bulk material responses. This is indeed our interest in the next step of this research.

ACKNOWLEDGEMENTS

This work was supported by CNPq (Conselho Nacional de Desenvolvimento Científico e Tecnológico) and FAPESP (São Paulo State Science Foundation) under the grants 303793/2012-0 and 2014/19821-7. respectively.

REFERENCES

Bathrust, R. J., 1985. *A study of stress and anisotropy in idealized granular assemblies*. PhD thesis, Queen's University/Canada.

Barreto, D., 2009. *Numerical and experimental investigation into the behaviour of granular materials under generalised stress states*. PhD thesis, University of London/London.

Cambou, B. et al., 2009. *Micromechanics of granular materials*. ISTE and John Wiley & Sons.

Cassares, K. R.; Campello, E. M. B. Characterization of the microstructure of randomly-generated particle packs for DEM Simulations of granular materials. *In: XXXVI Ibero-Latin American Congress on Computational Methods in Engineering (XXVI CILAMCE)*, 2015, Rio de Janeiro. v. s/n.

Campello, E. M. B., Cassares, K. R., 2016. Rapid generation of particle packs at high packing ratios for DEM simulations of granular compacts. *Lat. Amer. J. Sol. Struct.*

Chang, C. S., Chao, S. J., & Chang, Y., 1995. Estimates of elastic moduli fir granular material with anisotropic random packing structure. *Int. J. Solid and Struct.*, vol. 32, n. 4, pp. 1989–2008.

Cui, L., O'Sullivan, C., 2006.Exploring the macro- and microscale response of an idealised granular material in the direct shear apparatus. *Gèotechnique*, vol. 56, n. 7, pp. 455 – 468.

Cundall, P. A., & Strack, O. L., 1979. A discrete numerical model for granular assemblies. *Géotechnique*, vol. 29, n. 1, pp. 47–65.

Cundall, P. A. et al., 1982. Numerical experiments on granular assemblies; measurements and observations. In Vermeer, P. A., Luger, H. J., eds, *Deformation and Failure of Granular Materials*, pp. 355–370. Balkema, Rotterdam.

Darbre, G. R., & Wolf, J. P., 1985. Nonlinear elastic constitutive law for granular materials applicable to pebble-bed core. *Nuclear Engineering and Design*, vol. 88, n. 2, pp. 161–168.

Dorostkar, O., & Mirghasemi, A. A., 2016. Micro-mechanical study of stress path and initial conditions in granular materials using DEM. *Computational Particle Mechanics*, vol. 3, n. 1, pp. 15-27.

Emeriault, F., & Cambou, B., 1996. Micromechanical modelling of anisotropic non-linear elasticity of granular medium. *Int. J. Solids Structures*, vol. 33, n. 18, pp. 2591–2607.

Kruyt, N. P., 2012. Micromechanical study of fabric evolution in quasi-static deformation of granular materials. *Mechanics of Materials*, vol. 44, pp. 120–129.

Ng, T.-T., 1999. Fabric study of granular materials after compaction. *Journal of Engineering Mechanics*, vol. 125, n. 12, pp. 1309–1394.

Ng, T.-T., 2001. Fabric evolution of ellipsoidal arrays with different particle shapes. *Journal of Engineering Mechanics*, vol. 127, n. 10, pp. 994–999.

Ng, T.-T., 2004. Macro- and micro-behaviors of granular materials under different sample preparation methods and stress paths. *Int. J. Solid and Struct.*, vol. 41, n. 21, pp. 5871–5884.

Oda, M., 1972. The mechanism of fabric changes during compressional deformation of sand. *Soils and Found.*, vol. 12, n. 2, pp. 1–18.

O'Sullivan, C., 2011. *Particulate discrete element modelling – A geomechanics perspective*. Spon Press.

Rothenburg, L., 1980. *Micromechanics of idealized granular systems*. PhD thesis, Carleton University/Canada.

Rothenburg, L., & Bathrust, R. J., 1989. Analytical study of induced anisotropy in idealized granular materials. *Géotechnique*, vol. 39, n. 4, pp. 601–614.

Rothenburg, L., & Bathrust, R. J., 1992. Micromechanical features of granular assemblies with planar elliptical particles. *Géotechnique*, vol. 42, n. 2, pp. 79–95.

Rothenburg, L.; & Kruyt, N. P., 2004. Critical state and evolution of coordination number in simulated granular materials. *International Journal of Solids and Structure*, vol. 41, n. 21, pp. 5763–5774.

Shertzer, R. H., 2011. *Fabric tensors and effective properties of granular materials with application to snow*. PhD thesis, Montana State University/Montana.

Thornton, C., & Barnes, D. J., 1986. Computer Simulated Deformation of Compact Granular Assemblies. *Acta Mechanica*, vol. 64, n. 1-2, pp. 45–61.

Thornton, C.; & Antony, S. J., 1998. Quasi-static deformation of particulate media. *Phil. Trans. R. Soc. Lond A*, n. 356, n. 1747, pp. 2763–2782.

Thornton, C., 2000. Numerical simulations of deviatoric shear deformation of granular media. *Géotechnique*, n. 50, n. 1, p. 43–53.